Journal of Nanoscience and Nanotechnology
Vol. 18, 7512–7515, 2018
www.aspbs.com/jnn

InP-Based Coupled Ridge Waveguide Laser Arrays Emitting at 2.1 μm

Zhongkai Zhang[1,2], Feng Xu[1,2,3], Jinchuan Zhang[1,2], Zunren Lv[1,2], Xiaoguang Yang[1,2], Zhanguo Wang[1,2], and Tao Yang[1,2,*]

[1] Key Laboratory of Semiconductor Materials Science, Institute of Semiconductors, Chinese Academy of Sciences, Beijing 100083, China
[2] College of Materials Sciences and Opto-Electronic Technology, University of Chinese Academy of Sciences, Beijing, 100049, China
[3] Yangtze Memory Technologies Co., Ltd., Wuhan, 430205, China

We report on the first fabrication and characterization of InP-based coupled ridge waveguide laser arrays emitting at 2.1 μm. A dual-lobe far-field distribution in the lateral direction from the laser arrays is observed, indicating the far-field coherent coupling between the adjacent ridges. Meanwhile, a large peak output power of more than 2 W per facet is achieved at 15 °C. The compact structure and simple fabrication processes of the coupled ridge waveguide laser arrays make it a very promising approach to realize high power lasers with good beam quality for practical applications.

Keywords: Coupled Ridge Waveguide Laser Arrays, Quantum Well, Ridge Waveguides, Semiconductor Lasers.

1. INTRODUCTION

High performance lasers emitting from 2 to 2.5 μm are of high value for applications such as free space communication, gas detection, biomedicine, military fields, and so on.[1–4] In terms of this band, InP-based lasers with InGaAs multi-quantum wells (MQWs) are highly preferred for its low cost, high quality, and mature fabrication technology. In order to achieve the requirements for practical applications, both high output power and high beam quality are needed. The most conventional approach to get high power is to increase the width of ridge to expand the lasing area. However, broad ridge lasers tend to produce a poor beam quality, resulting from multiple lateral modes operation.[5] New concepts such as master-oscillator power-amplifiers[6] and angled cavity lasers[7] have been put forward in recent years to realize high power lasers and showed excellent performance, but their structures are quite complicated simultaneously. In contrast, the coupled ridge waveguide laser arrays, whose structures are compact and the fabrication process is simple, are attractive to many researchers.[8–15] By this means, the devices can modulate the lateral mode characteristics based on the differences of effective refractive index between injected and etched regions, leading to a better beam quality and a high output power comparable to conventional devices with broad ridges. So far, extensive research has been in progress in terms of near-infrared lasers[9,12] and quantum cascade lasers;[10,14] and here we attempt to introduce this structure to our InP-based lasers emitting at the band of 2 μm.

In this work, an InP-based coupled ridge waveguide laser arrays consisting of sixteen ridge elements is designed and fabricated. A dual-lobe far-field distribution in the lateral direction is observed, implying the far-field coherent coupling between adjacent emitting regions is realized. The device can work stably from 15 to 105 °C under pulsed injection and it shows a large peak output power of more than 2 W from one facet at 15 °C under an injection current of 10 A, with a threshold current and slope efficiency of 0.57 A and 0.5 W/A, respectively.

2. EXPERIMENTAL DETAILS

The laser structure was grown on an n-type (100)-InP substrate by an AIXTRON 3 × 2 FT Metalorganic Vapor Phase Epitaxy (MOVPE) system. The active region was a separate confinement hetero-structure (SCH) MQWs, which consisted of two 5-nm-thick InAs wells and three 20-nm-thick $In_{0.53}Ga_{0.47}As$ barriers. The confinement waveguide layers were 200-nm-thick InGaAsP films with a bandgap

*Author to whom correspondence should be addressed.

1533-4880/2018/18/7512/004 doi:10.1166/jnn.2018.16087

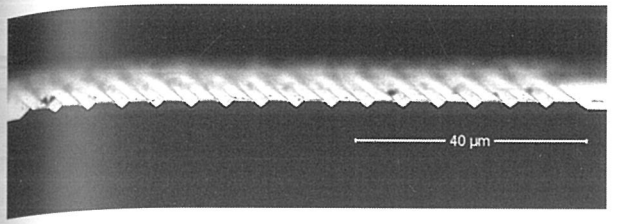

Figure 1. Scanning electron microscopy image of coupled ridge waveguide laser arrays.

wavelength of 1.2 μm. The detailed growth conditions can be found elsewhere.[16]

After the growth of the laser structure, a series of fabrication processes were followed. Firstly, the ridge waveguide laser arrays were formed by photolithography and wet etching. The proposed coupled ridge waveguide laser arrays structure consists of sixteen ridge elements with an average width of about 4 μm and a center-to-center spacing of 6 μm, with a total array width of 96 μm (as shown in Fig. 1). The etching depth of the interspace was about 1.7 μm. Then, a 350-nm-thick SiO_2 layer was deposited by Plasma Enhanced Chemical Vapor Deposition (PECVD) and the ohmic contact window was opened. The electrode contact was provided by a Ti/Au layer, which was followed by thinning the substrate to about 90 μm. Next, a Ge/Au/Ni/Au metal contact layer was deposited on the back side of the wafer. After alloyed in N_2 atmosphere, the wafer was cleaved into bars with cavity length of 1.5 mm.

The laser was then bonded down to a copper heat sink with Indium solder for testing. The output power of the laser was measured by a calibrated thermopile detector located in front of the laser facet. A thermoelectric cooler (TEC) was outfitted to control the temperature of the heat sink. The injection current for pulsed measurements was set at 1% duty cycle with 2 μs pulse width. Emission spectrum of the laser was measured by a THORLABS Optical Spectrum Analyzer 203 and the heat sink temperature of the laser was maintained at 25 °C during the test. Subsequently, the laser was mounted on a computer-controlled stage, which can rotate with a step resolution of 0.05°, and the far-field measurement was taken. For collecting the emission light of the laser, a nitrogen-cooled HgCdTe detector was used and placed in front of the stage.

3. RESULTS AND DISCUSSION

The electrical characteristic of the device was firstly investigated. The injection current was set at 1% duty cycle with 2 μs pulse width, from 0 to 10 A and the test temperature was maintained at 15 °C. Both facets of the device were uncoated. As shown in Figure 2, the device exhibits a large peak output power of more than 2 W (2.17 W) for one facet with the threshold current and slope efficiency of 0.57 A and 0.5 W/A (for two facets), respectively. Emission characteristic of the device was measured

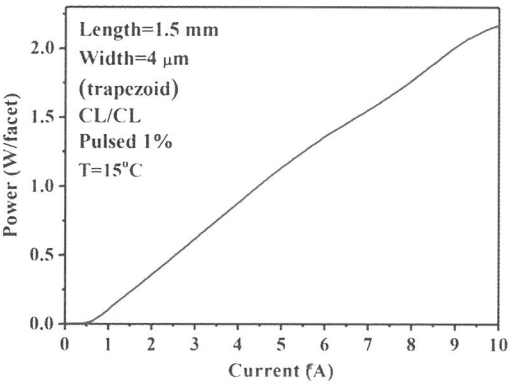

Figure 2. Light-current curve under pulsed injection with the heat sink temperature maintained at 15 °C.

subsequently. The measurement was carried out under continuous wave injection, with the injection current of 1 A. Figure 3 shows the emission spectrum pattern of the coupled ridge waveguide laser arrays, where the emission wavelength of the laser is at 2162 nm.

Subsequently, measurements for the temperature characteristic were carried out. The test temperature was controlled to vary from 15 to 105 °C, with a stepped temperature interval of 10 °C. The injection current was set at 1% duty cycle with 2 μs pulse width, from 0 to 6 A. Figure 4 presents the light-current curves of the coupled ridge waveguide laser arrays under different temperatures. As the temperature increases, the maximum peak output power of the device from one facet changes gradually from 1360 to 127 mW at the injection current of 6 A, but is still larger than 100 mW even at 105 °C, which indicates that the device has a good output power characteristic at the given temperature range. The threshold current and slope efficiency changed from 0.57 to 3.66 A and 0.5 to 0.1 W/A for the different testing temperatures from 15 to 105 °C, respectively, due to the enhanced thermal escaping of carriers from the QWs and auger recombination at higher temperatures. We can find in Figure 4 that the threshold current and slope efficiency vary relatively slowly when the temperature is smaller

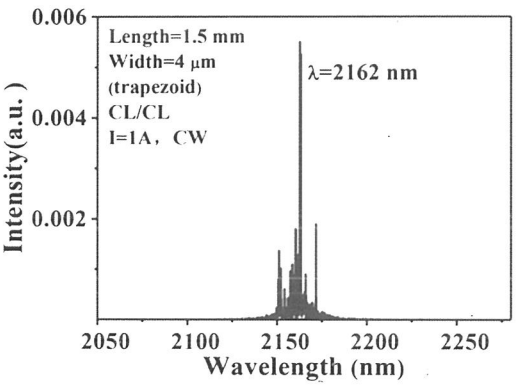

Figure 3. Spectrum of coupled ridge waveguide laser arrays.

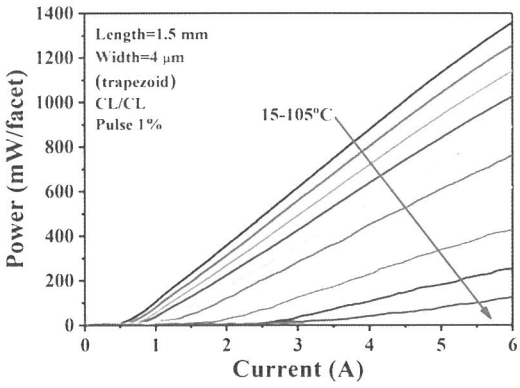

Figure 4. Light-current curves of coupled ridge waveguide laser arrays under pulsed injection with different heat sink temperatures varying from 15 to 105 °C.

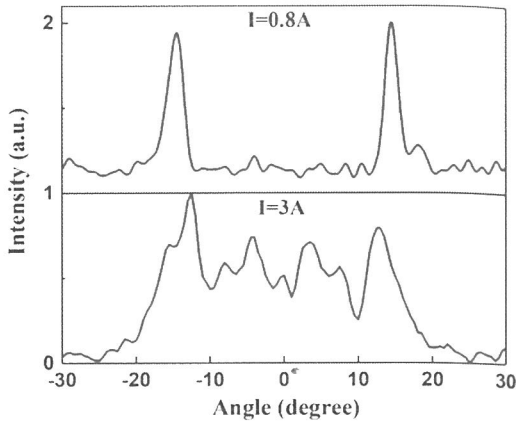

Figure 6. Far-field radiation patterns of coupled ridge waveguide laser arrays under different injections.

than 75 °C. Figure 5 plots the threshold current and the slope efficiency as a function of temperature, where the characteristic temperature (T_0) of the laser is 65 K and 39 K between the temperatures of 15 °C to 75 °C and between the temperatures of 75 °C to 105 °C, respectively; while the temperature characteristic (T_1) regard to the slope efficiency is 106 K (15 to 75 °C) and 31 K (75 to 95 °C), respectively.

Figure 6 shows the lateral far-field pattern of the coupled ridge waveguide laser arrays. The injection current was set at 2% duty cycle with 2 μs pulse width. As observed in Figure 6, when the injection current is 0.8 A, there are two narrow peaks with the full width at half maximum (FWHM) of 2.61° and 2.05°, respectively, which are about 1.83 and 1.43 times the diffraction limited (i.e., 1.43° for an in-phase coupled ridge waveguide laser arrays emitting at 2.1 μm with a total array width of 96 μm). Hence, we believe that the far-field coherent coupling between adjacent emitting regions has been realized in the laser. However, the coupled ridge waveguide laser arrays show a dual-lobe far-field distribution in the lateral direction, indicating the high-order super-mode operation of the laser instead of the fundamental super-mode. We attribute it to the higher modal gain of the high-order mode compared with the fundamental super-mode, and the laser prefers to lase at high-order mode as a consequence. Moreover, when increasing the injection current to 3 A, multiple high-order super-modes lased simultaneously, making the far-field pattern a mixture of several lobes corresponding to these super-modes. To realize fundamental super-mode operation and single-lobe far-field distribution at high injection level, further optimizing of the structure is needed.

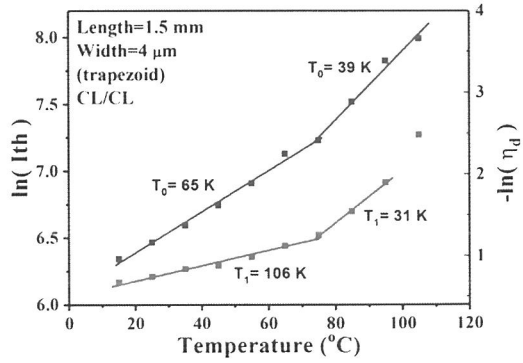

Figure 5. Temperature dependence of threshold and slope efficiency characteristics.

4. CONCLUSION

In conclusion, we have fabricated and characterized the InP-based coupled ridge waveguide laser arrays emitting at 2.1 μm, which consists of sixteen ridge elements. The lateral far-field pattern from the laser arrays shows a dual-lobe distribution, indicating the existence of coherent coupling between adjacent emitting regions. Stable operation from 15 to 105 °C under pulsed injections and a large peak output power of more than 2 W from one facet with a threshold current and slope efficiency of 0.57 A and 0.5 W/A at 15 °C are achieved. The compact structure and simple fabrication processes effectively increase the repeatability and reduce the cost of the devices, making it have huge potential and broad prospects in practical applications.

Acknowledgments: This work was supported by the National Natural Science Foundation of China under Grants 61574139 and the National Key Research and Development Program of China under Grant No. 2017YFB0405302. And the authors would like to thank Dr. N. Zhuo for beneficial discussions and their great help on the design of device structure.

References and Notes

1. R. W. Waynant, I. K. Ilev, and I. Gannot, *Philos. Trans. Roy. Soc. B Biological Sciences* 359, 635 (**2001**).
2. A. Godard, *Comptes Rendus Physique* 8, 1100 (**2007**).

3. W. Lei and C. Jagadish, *J. Appl. Phys.* 104, 11 **(2008)**.
4. H. Yang, N. Ye, R. Phelan, J. O'Carroll, B. Kelly, W. Han, X. Wang, N. Nudds, N. Macsuibhne, and F. Gunning, *Electronics Letters* 49, 281 **(2013)**.
5. B. Sumpf, M. Zorn, M. Maiwald, R. Staske, J. Fricke, P. Ressel, G. Erbert, M. Weyers, and G. Trankle, *IEEE Photonics Technology Letters* 20, 575 **(2008)**.
6. O. Brox, F. Bugge, A. Ginolas, A. Klehr, P. Ressel, H. Wenzel, G. Erbert, and G. Tränkle, *Proc. SPIE* 7616, 761610 **(2010)**.
7. Y. Bai, S. Slivken, Q. Y. Lu, N. Bandyopadhyay, and M. Razeghi, *Appl. Phys. Lett.* 101, 941 **(2012).**
8. H. Streifer, R. D. Burnham, and D. R. Scifres, *Electron. Lett.* 21, 118 **(1984)**.
9. D. R. Scifres, R. D. Burnham, and W. Streifer, *Appl. Phys. Lett.* 33, 1015 **(1978)**.
10. F. L. Yan, J. C. Zhang, Z. W. Jia, N. Zhuo, S. Q. Zhai, S. M. Liu, F. Q. Liu, and Z. G. Wang, *Aip Advances* 6, 553 **(2016)**.
11. D. Botez and J. C. Connolly, *Appl. Phys. Lett.* 43, 1096 **(1983)**.
12. Y. Twu, A. Dienes, S. Wang, and J. R. Whinnery, *Appl. Phys. Lett.* 45, 709 **(1984)**.
13. D. Scifres, W. Streifer, and R. Burnham, *IEEE Journal of Quantum Electronics* 15, 917 **(1979)**.
14. Y. H. Liu, J. C. Zhang, F. L. Yan, F. Q. Liu, N. Zhuo, L. J. Wang, J. Q. Liu, and Z. G. Wang, *Appl. Phys. Lett.* 106, 553 **(2015)**.
15. G. M. D. Naurois, M. Carras, B. Simozrag, O. Patard, F. Alexandre, and X. Marcadet, *Aip Advances* 1, 181102 **(2011)**.
16. S. Luo, H. M. Ji, F. Gao, F. Xu, X. G. Yang, P. Liang, and T. Yang, *Opt. Express* 23, 8383 **(2015)**.

Received: 18 January 2018. Accepted: 24 March 2018.